

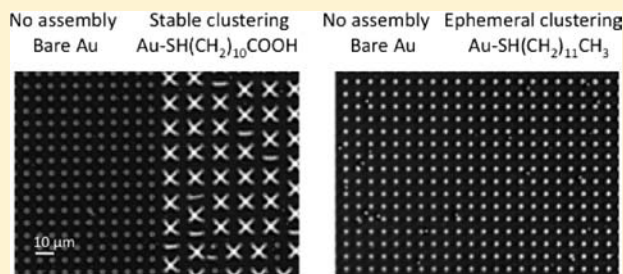
# Controlling the Stability and Reversibility of Micropillar Assembly by Surface Chemistry

Mariko Matsunaga,<sup>†,‡</sup> Michael Aizenberg,<sup>‡</sup> and Joanna Aizenberg<sup>\*,†,‡,§</sup>

<sup>†</sup>School of Engineering and Applied Sciences, <sup>‡</sup>Wyss Institute for Biologically Inspired Engineering, and <sup>§</sup>Department of Chemistry and Chemical Biology, Harvard University, Cambridge, Massachusetts 02138, United States

**S** Supporting Information

**ABSTRACT:** For many natural and synthetic self-assembled materials, adaptive behavior is central to their function, yet the design of such systems has mainly focused on the static form rather than the dynamic potential of the final structure. Here we show that, following the initial evaporation-induced assembly of micropillars determined by the balance between capillarity and elasticity, the stability and reversibility of the produced clusters are highly sensitive to the adhesion between the pillars, as determined by their surface chemistry and further regulated by added solvents. When the native surface of the epoxy pillars is masked by a thin gold layer and modified with monolayers terminated with various chemical functional groups, the resulting effect is a graded influence on the stability of cluster formation, ranging from fully disassembled clusters to an entire array of stable clusters. The observed assembly stabilization effect parallels the order of the strengths of the chemical bonds expected to form by the respective monolayer end groups:  $\text{NH}_2 \approx \text{OH} < \text{COOH} < \text{SH}$ . For each functional group, the stability of the clusters can be further modified by varying the carbon chain length of the monolayer molecules and by introducing solvents into the clustered samples, allowing even finer tuning as well as temporal control of disassembly. Using these features together with microcontact printing, we demonstrate straightforward patterning of the microstructured surfaces with clusters that can be erased and regenerated at will by the addition of appropriate solvents. Subtle modifications to surface and solvent chemistry provide a simple way to tune the balance between adhesion and elasticity in real time, enabling structures to be designed for dynamic, responsive behavior.



## 1. INTRODUCTION

While some self-assembled systems are designed to remain stable under changing conditions, the function of many others requires them to associate and dissociate in response to specific environmental cues. In nature, relatively stable assemblies of lipid bilayer components, of cytoskeletal fibers, and of cells are essential to the structural integrity of cells and tissues.<sup>1</sup> At the same time, various protein assemblies partially open to transport ions,<sup>2–4</sup> sugars,<sup>5</sup> vitamins,<sup>6</sup> and proteins<sup>7</sup> and to transduce signals; DNA unwinds to allow replication; and polymeric actin filaments add and subtract monomers to enable cell motility. Beyond biochemistry, ordered self-assembly systems attract materials scientists for their wide range of potential applications in photonic and microelectronic materials, economical manufacture of robotics, and bottom-up nanotechnology.<sup>1</sup> The ability to control and regulate the stability of such systems and to induce their reversible assembly and reconfiguration would greatly enhance their potential applications for dynamic functionalities, possibly even approaching the sophistication level of those observed in nature. To achieve that, one should go beyond the limitation of the common designs that mostly focus on how to create particular static structures through irreversible self-organization or fabrication rather than on controlling their ability to dynamically reorganize the assembled structures. Optimizing

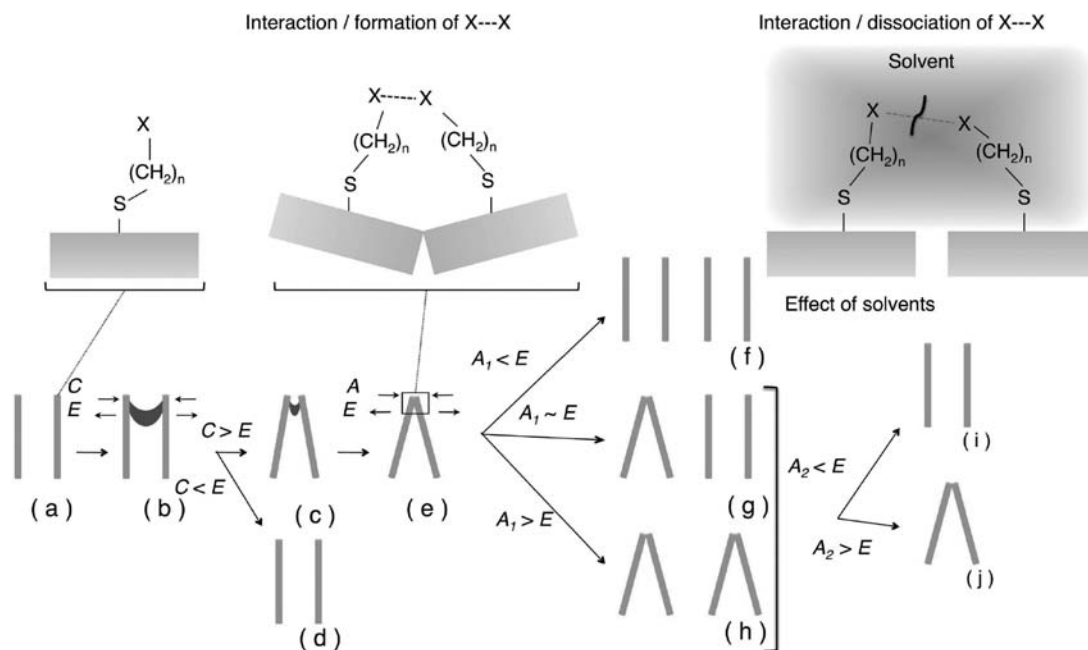
these features requires temporal tuning of the balance between attractive and repulsive forces.

Arrays of high-aspect-ratio nano/micropillars found in nature display unique properties, such as the superhydrophobicity of the legs of water striders,<sup>8,9</sup> the reversible adhesion of the gecko's foot,<sup>10</sup> reassembly of the segmented leg (tarsi) of the beetle *Hemisphaerota cyanea*,<sup>11</sup> attachment systems of various other insects,<sup>12,13</sup> and the coordinated motion used by cilia for controlling cell motility, removing viruses, and sensing.<sup>14–18</sup> Reversible assembly of the pillars can switch or gradually change physical, chemical, biological, and mechanical properties of the array by changing its exposed surfaces and overall structure and can enable it to capture particles between pillars and release them when needed.

Previous studies demonstrated that capillary effects can be utilized to form a variety of two- and three-dimensional structures from arrays of pillars assembling in an evaporating liquid at the nano- to macroscales.<sup>19–34</sup> While the size and pattern of the assembly were described to be controlled by the interplay between capillarity and elasticity alone, our recent report analyzing the high-order clustering of epoxide nanopillars in

Received: January 10, 2011

Published: March 22, 2011

Scheme 1. Experimental System<sup>a</sup>

<sup>a</sup> Micropillars are initially in an upright position and do not interact (a). During solvent evaporation (b), pillars are brought together (c) if the capillary force  $C$  that drives bending is stronger than the restoring elastic force  $E$  ( $C > E$ ), but are left standing (d) if  $C < E$ . After the solvent dries,  $C$  is lost and the only force opposing  $E$  is the adhesion force  $A$  (e). Intermolecular bonds between assembled pillars are expected to have formed at this stage and to contribute to  $A$ . Clusters will disassemble if  $A_1 < E$  (where  $A_1$  denotes interpillar adhesion resulting from exposure to Solvent 1) (f); be only moderately stable if  $A_1 \approx E$  (g); or be very stable if  $A_1 > E$  (h). Introduction of Solvent 2 to stable clusters can change adhesion ( $A_1 \rightarrow A_2$ ) by altering the bonding network between pillars. Solvent 2 will induce disassembly if  $A_2 < E$  (i), but clusters will remain stable if  $A_2 > E$  (j). For the array of pillars, the magnitude of  $A_1$  or  $A_2$  relative to  $E$  is directly read out as the percentage of stable clusters, allowing quantitative comparison of the adhesion force for different surface modifications and chemical environments.

evaporating liquid<sup>32</sup> pointed toward the importance of adhesion in determining the stability and therefore the size of the final assemblies. This raises a fascinating possibility of using adhesion as a means to regulate the assembly process. Adhesion is influenced by many factors<sup>35</sup> including mechanical interlock, adsorption, chemisorption, electrostatics, and diffusion. We hypothesize that by controlling the adhesive properties of micropillars via chemical modification of their surfaces one can tune the interaction between assembling pillars and make it dynamic and environment-responsive. In the present study, we directly and systematically examine the role of adhesion in evaporation-induced micropillar clustering and demonstrate that manipulating the surface chemistry of the pillars — in particular the functional end groups of self-assembled monolayers (SAMs) covering the pillars, length of carbon chains of the SAMs, and exposure of the pillars to various solvents — can serve as a simple, easily tunable way to control the stability and reversibility of the assembly process.

## 2. EXPERIMENTAL SECTION

### 2.1. Preparation of Arrays of Polyepoxide Micropillars.

Micropillars (diameter:  $1.5 \mu\text{m}$ , pitch:  $8 \mu\text{m}$ , height:  $10 \mu\text{m}$ ) made of epoxy resin (UVO114, Epoxy Technology) were prepared by the soft lithographic method from a PDMS negative mold. UVO 114 was poured into the PDMS mold and cured by UV exposure for 20 min. Preparation of the PDMS negative mold was described in detail previously.<sup>36</sup> The root-mean-square roughness of the thus prepared flat epoxy surface was  $1.9 \text{ nm}$  for a  $1 \mu\text{m} \times 1 \mu\text{m}$  area and  $2.8 \text{ nm}$  for a  $10 \mu\text{m} \times 10 \mu\text{m}$  area.

**2.2. Surface Modification and Characterization.** The entire surfaces of the pillars were sputter-coated with a layer of Au with a thickness of  $100 \text{ \AA}$ . The Au deposition rate was  $1 \text{ \AA/s}$ . To ensure adhesion of Au to the epoxy surface, a titanium film having a thickness of less than  $60 \text{ \AA}$  was used as an adhesion layer. The root-mean-square roughness of the thus prepared Au-sputtered flat epoxy surface was  $2.1 \text{ nm}$  for the  $1 \mu\text{m} \times 1 \mu\text{m}$  area and  $6.0 \text{ nm}$  for the  $10 \mu\text{m} \times 10 \mu\text{m}$  area. The surfaces were then modified at room temperature by the following methods: (i) immersing the sample in a  $1 \text{ mM}$  ethanol solution of thiol molecules for 1 h (Method I), (ii) vapor deposition for 3 days (Method II), or (iii) soft contact with a PDMS stamp inked with a  $1 \text{ mM}$  thiol solution for 1 h (Method III). After rinsing with ethanol, the surfaces were dried in air.

Cysteamine ( $\text{SH}(\text{CH}_2)_2\text{NH}_2$ , thereafter referred to as  $\text{C}_2\text{-NH}_2$ ), 3-Mercapto-1-propanol ( $\text{SH}(\text{CH}_2)_3\text{OH}$ ,  $\text{C}_3\text{-OH}$ ), 11-Mercapto-1-undecanol ( $\text{SH}(\text{CH}_2)_{11}\text{OH}$ ,  $\text{C}_{11}\text{-OH}$ ), 3-Mercaptopropionic acid ( $\text{SH}(\text{CH}_2)_2\text{COOH}$ ,  $\text{C}_2\text{-COOH}$ ), 11-Mercaptoundecanoic acid ( $\text{SH}(\text{CH}_2)_{10}\text{COOH}$ ,  $\text{C}_{10}\text{-COOH}$ ), 1,2-Ethanedithiol ( $\text{SH}(\text{CH}_2)_2\text{SH}$ ,  $\text{C}_2\text{-SH}$ ), 1,9-Nonanedithiol ( $\text{SH}(\text{CH}_2)_9\text{SH}$ ,  $\text{C}_9\text{-SH}$ ), and 1-Dodecanethiol ( $\text{SH}(\text{CH}_2)_{11}\text{CH}_3$ ,  $\text{C}_{11}\text{-CH}_3$ ) used for surface modification were purchased from Aldrich and used as received.

Contact angle (CA) measurements on the flat epoxy surfaces, chemically modified with Au and respective monolayer molecules, were performed using a CAM101 (KSV Instruments LTD) instrument. The CA for each thiol-modified surface is an average of two samples, each of which was measured on three areas for both the right and left sides. All contact angles were measured in air against DI water. Substrates were kept horizontal during the measurement.

**2.3. Examination of Clustering.** Clustering was examined by scanning electron microscopy (SEM) (JSM-6390LV, JEOL) and optical

microscopy (IX71, Olympus). All of the measurements were performed under ambient conditions. The percentage of clusters was determined for five areas of approximately  $400 \times 300 \mu\text{m}^2$  for each sample to obtain reliable statistics and standard deviations.

### 3. RESULTS

**3.1. System Design.** The experimental design is outlined in Scheme 1. In the dry state, when the capillary force ( $C$ ) is gone, only the adhesion force ( $A$ ) among the pillars remains to counteract the elastic force ( $E$ ). Since our previous studies<sup>29,32</sup> suggest that adhesion can have complex effects on the formation of high-order clusters (up to  $\sim 10 \times 10$  pillars), we deliberately reduce the complexity of the system such that the size of the clusters that can initially assemble in the evaporating liquid is not higher than  $2 \times 2$  (Scheme 1a–d). Thus we can read out the magnitude of the adhesion forces in a particular system simply by

**Table 1. Average Contact Angles of Water Droplets on Flat Au Surfaces Functionalized by SAMs, Measured in Air**

Surface	Contact Angle <sup>a</sup> /deg
Bare Au	$31 \pm 6.6$
C <sub>2</sub> -NH <sub>2</sub>	$38 \pm 6.9$
C <sub>3</sub> -OH	<10
C <sub>11</sub> -OH	$40 \pm 3.4$
C <sub>2</sub> -COOH	<10
C <sub>10</sub> -COOH	$28 \pm 4.3$
C <sub>2</sub> -SH	$67 \pm 10$
C <sub>9</sub> -SH	$92 \pm 11$
C <sub>11</sub> -CH <sub>3</sub>	$97 \pm 3.4$

<sup>a</sup> Each contact angle is an average value of 12 measurements.

quantifying the density of clusters that remain stable after the solvent dries, with an additional level of subtlety discernible by comparing relative numbers of  $1 \times 1$  and  $2 \times 2$  clusters (see Scheme 1 for details). This reductionist approach allows us to systematically vary and study the adhesion forces ( $A$ ) that are at play.

Structures satisfying these conditions consisted of an array of micropillars  $1.5 \mu\text{m}$  in diameter with a pitch of  $8 \mu\text{m}$  and a height of  $10 \mu\text{m}$ , made of epoxy resin UVO114 (Epoxy Technology).<sup>29,37</sup> We hypothesized that in such a system, after the initial clustering in the presence of a solvent, we would be able to observe and quantify the degree of cluster retention (or, conversely, disassembly) that would take place on drying or immersion in a different solvent, as a direct measure of the adhesion force among the micropillars for each type of surface modification and environment (Scheme 1f–j). To study a variety of possible chemical interactions and their effect on the macroscopic adhesion among (and between) the micropillars, we chose to chemically functionalize the pillars' surface with a number of modifier molecules that included short- and longer-chain thiols with a range of functional end groups (see the Experimental Section above). The contact angle data, which provide chemical characterization of hydrophobicity/phillicity of surfaces, for the flat gold-covered surfaces functionalized using Method I are given in Table 1. The following section describes the results obtained for each specific type of chemical functionalization we studied.

**3.2. Chemical Modification of the Pillars by SAMs and Its Effect on Cluster Stability.** Since nonmodified epoxy micropillars are intrinsically able to form stable clusters by capillary-induced self-assembly,<sup>32,36</sup> we coated the entire surface of the pillars with a thin gold film to cancel any contribution to the adhesion from the native chemical surface properties. All the subsequent studies and chemical surface modifications were

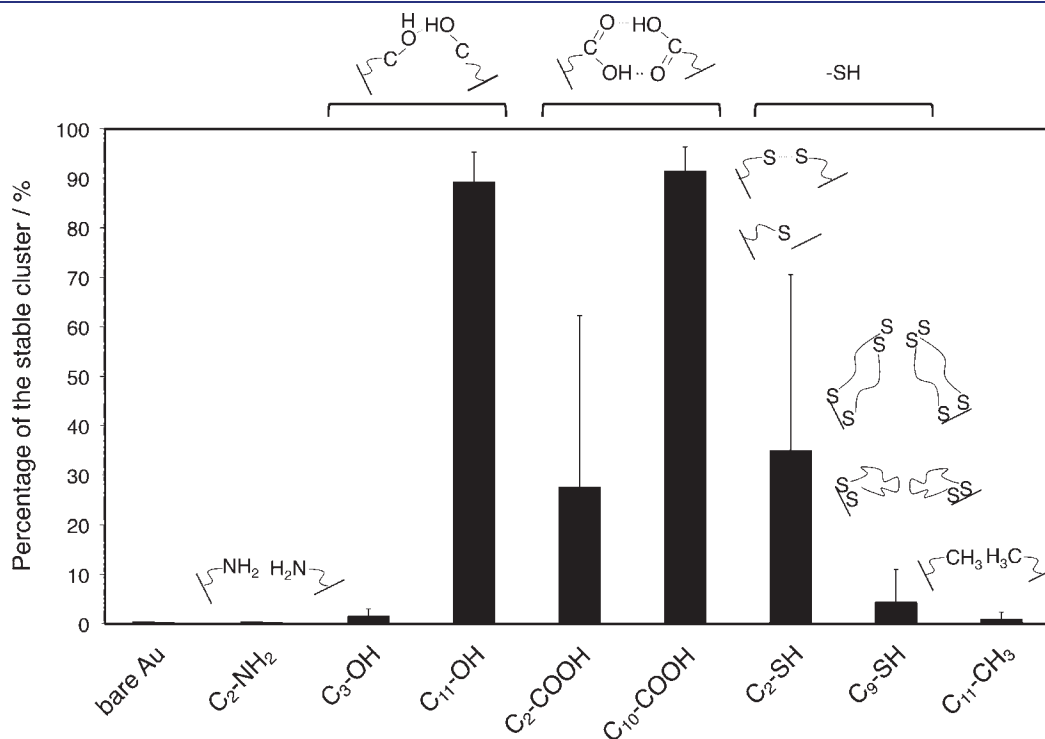


**Figure 1.** Percentage of stable clusters observed after drying of ethanol for pillar arrays coated with Au with or without functionalization with various thiol molecules. Error bars are shown as +standard deviation.

performed using pillars that had been precoated with such a gold layer. The observations and statistical characterizations of the stable clusters described below were made after the solvent usually used for chemical modification and rinsing of the surface (ethanol, unless otherwise specified) had evaporated. The results are presented qualitatively as representative micrographs and quantitatively as the percentage of pillars that formed stable clusters.

When the nonfunctionalized Au-coated pillar array was immersed in ethanol, dried in air, and subsequently examined by microscopy, no clusters were observed (Figure 1) and the array looked the same as before the treatment (Figure 2a). An almost identical result was observed for the pillars modified, using Method I, with a methyl-terminated alkylthiol,  $C_{11}\text{-CH}_3$  (Figures 1 and 2i). Importantly, however, in the latter case, capillarity-induced clustering did initially take place at the stage when ethanol was still present, but on drying, all the formed four-pillar clusters spontaneously disassembled (Figure 3). This

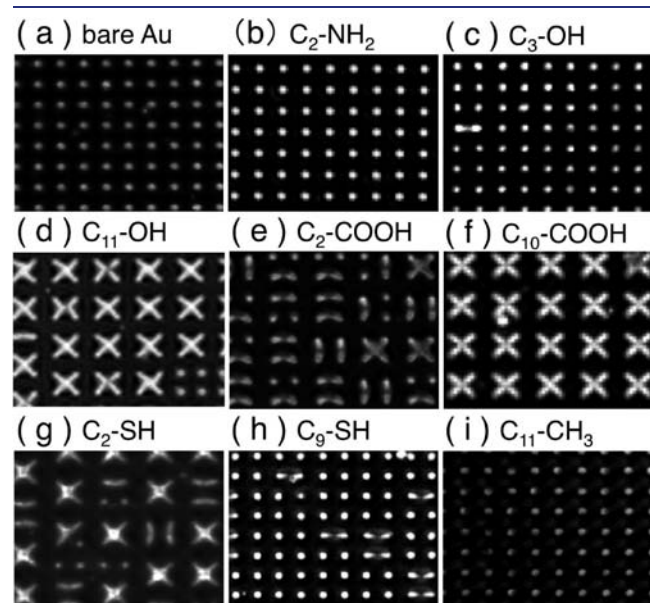


**Figure 2.** Optical microscopic images (top views) of pillar arrays modified with SAMs after rinsing with ethanol and drying. (a) Bare Au, (b) Cysteamine ( $C_2\text{-NH}_2$ ), (c) 3-Mercapto-1-propanol ( $C_3\text{-OH}$ ), (d) 11-Mercapto-1-undecanol ( $C_{11}\text{-OH}$ ), (e) 3-Mercaptopropionic acid ( $C_2\text{-COOH}$ ), (f) 11-Mercaptoundecanoic acid ( $C_{10}\text{-COOH}$ ), (g) 1,2-Ethanedithiol ( $C_2\text{-SH}$ ), (h) 1,9-Nonanedithiol ( $C_9\text{-SH}$ ), and (i) 1-Dodecanethiol ( $C_{11}\text{-CH}_3$ ). Frame dimensions are  $80\ \mu\text{m} \times 60\ \mu\text{m}$ .

behavior is presented in Supporting Movie 1<sup>38</sup> and further elaborated upon in the Discussion section. Only a very small percentage ( $\sim 1\text{--}5\%$ ) of stable clusters was observed when the gold surface covering the pillars was functionalized, using Method I, with Cysteamine ( $C_2\text{-NH}_2$ ), 3-Mercapto-1-propanol ( $C_3\text{-OH}$ ), or Nonanedithiol ( $C_9\text{-SH}$ ) (Figure 1). In fact, almost all of the pillars that initially formed four-pillar ephemeral clusters returned on drying to their initial upright position, except for a very small number of two-pillar clusters that remained stable for  $C_3\text{-OH}$  and  $C_9\text{-SH}$ , as shown in Figure 2b, c, h.

In sharp contrast to the above cases, functionalization of the pillars' surface with 11-Mercapto-1-undecanol ( $C_{11}\text{-OH}$ ) or 11-Mercaptoundecanoic acid ( $C_{10}\text{-COOH}$ ) led to almost complete ( $>90\%$ ) stable clustering (Figure 1). The  $C_{10}\text{-COOH}$ -functionalized surface produced an almost uniform field of four-pillar clusters (Figure 2f), while functionalization with  $C_{11}\text{-OH}$  resulted in almost all four-pillar clusters with a small percentage of partially or fully disassembled clusters (Figure 2d). We note that, for pillars modified with  $C_{10}\text{-COOH}$ , the same result was observed whether they had been functionalized by Method I (from ethanol solution) or by Method II (from the vapor phase), while a mock modification reaction using ethanol alone did not produce any clusters.

The remaining two of the thiols that we used in the functionalization experiments, namely 1,2-Ethanedithiol ( $C_2\text{-SH}$ ) and 3-Mercaptopropionic acid ( $C_2\text{-COOH}$ ), led to an intermediate degree of clustering (25–35%, Figure 1).  $C_2\text{-SH}$  cluster sizes were equally distributed between four- and two-pillar clusters (Figure 2g), while  $C_2\text{-COOH}$  clusters were predominantly two pillars with a smaller contribution of clusters of four (Figure 2e).

**3.3. Effects of Solvents on the Adhesion between Clustered Pillars.** In order to probe the robustness of the clustered systems described above and to obtain additional information regarding the nature and strength of the adhesion forces at play in each particular case, we treated the dry clustered micropillar samples with a range of solvents. We found that the stable clusters formed in the micropillar systems functionalized with  $C_{11}\text{-OH}$ ,  $C_2\text{-COOH}$ , and  $C_{10}\text{-COOH}$  were easily disassembled by water or organic solvents, such as ethanol, acetone, and chloroform. The rate of disassembly of the clusters decreased in the order roughly following the increase of the dielectric constant of the solvent: chloroform (fastest rate)  $\gg$  acetone  $>$  ethanol  $\approx$  water (slowest rate).<sup>39</sup> In sharp contrast, the clusters formed in the case of  $C_2\text{-SH}$  remained clustered, even after prolonged rinsing with these solvents. Significantly, after the solvent-induced disassembly, the clusters could be easily

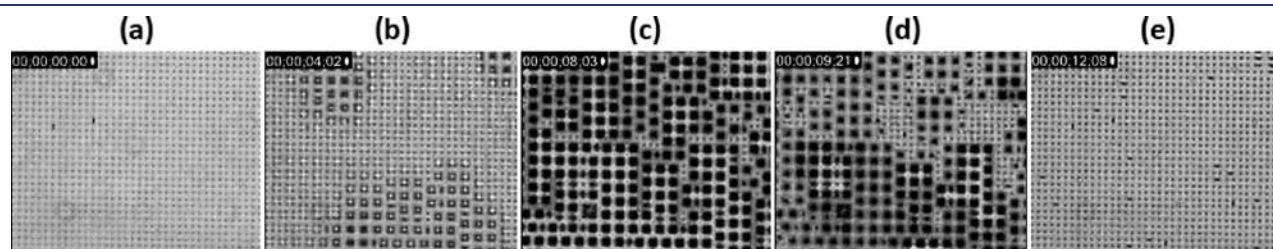


**Figure 3.** Still frames from the Supporting Movie 1<sup>38</sup> showing capillarity-induced clustering of the micropillar array functionalized with  $C_{11}\text{-CH}_3$  and its disassembly upon drying. (a) Micropillar array fully submerged in ethanol. (b) As ethanol level reaches the tips of the pillars, assembly into  $2 \times 2$  clusters is initiated. (c) Prior to the complete evaporation of ethanol, fully clustered micropillar arrays composed predominantly of  $2 \times 2$  clusters are formed. (d) Upon further evaporation of ethanol, these ephemeral clusters begin to disassemble at the dry regions. (e) Full disassembly of the micropillar clusters occurs after the complete evaporation of ethanol; in the dry state the posts return to the initial upright position. Frame dimensions are  $300\ \mu\text{m} \times 240\ \mu\text{m}$ .

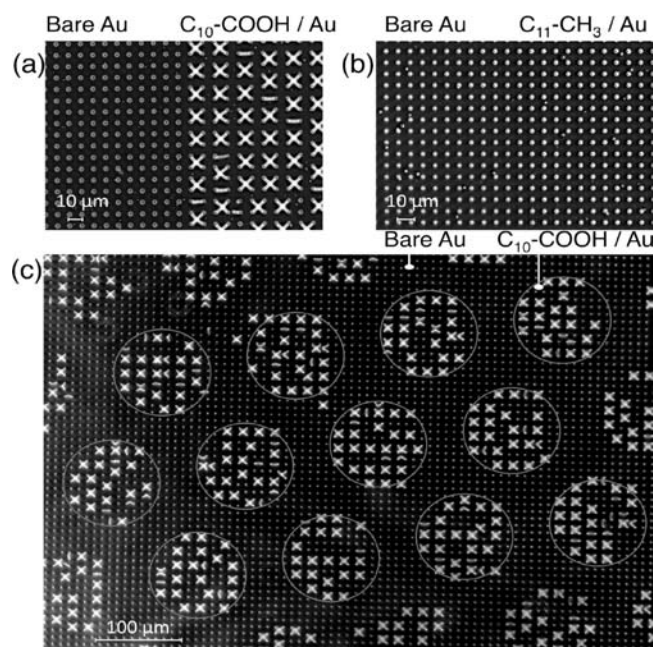


**Figure 4.** Patterning of the clusters by stamping 11-Mercaptoundecanoic acid ( $C_{10}$ -COOH) or 1-Dodecanethiol ( $C_{11}$ -CH<sub>3</sub>) on gold using microcontact printing. (a) Only the right half is modified by  $C_{10}$ -COOH. (b) The right half is modified by  $C_{11}$ -CH<sub>3</sub>. (c) Patterning of  $C_{10}$ -COOH in an array of circles. White outlines indicate the stamped areas (diameter: 100  $\mu$ m).

reformed by simply resubjecting the samples to treatment with ethanol and drying.

**3.4. Reversible Area-Selective Clustering.** The results of solvent effects on the stability of the clusters described in the previous section allowed us to utilize this knowledge to achieve reversible patterned clustering with precise spatial and temporal control. First, the tips of the Au-covered polyepoxide pillars were locally printed with a thiol-/ethanol-dipped stamp. Subsequently, cluster assembly was induced by rinsing with and gradual evaporation of ethanol. Figure 4 shows optical microscopy images of gold-coated pillars (a) half-patterned with  $C_{10}$ -COOH, (b) half-patterned with  $C_{11}$ -CH<sub>3</sub>, and (c) patterned with 100  $\mu$ m diameter circles of  $C_{10}$ -COOH. Clustering was induced *only* in the areas printed with  $C_{10}$ -COOH. Importantly, rinsing the clustered surface with chloroform could easily erase this patterning, and the pattern could be regenerated by retreatment with ethanol and drying as demonstrated before (Figure 5). This reproducible, reversible switching between erasing and reforming of the patterned clusters can be clearly seen in Supporting Movie 2.<sup>38</sup>

## 4. DISCUSSION

**4.1. Chemical Surface Modification As a Handle on Adhesion.** For the following detailed discussion of the phenomena involved in the micropillar clustering, we refer, again, to Scheme 1. In the designed micropillar system (Scheme 1a), when the ethanol solution of a chemical modifier (various thiols in our case) is introduced (Scheme 1b), the balance between the capillary force  $C$  and the elastic force  $E$  determines whether the pillars will remain standing in the upright position ( $C < E$ , Scheme 1d) or bend to form clusters ( $C > E$ , Scheme 1c). If the

solution contains chemical modifiers capable of reacting with the gold surface, the chemical functionalization of the surface takes place. When thus chemically functionalized pillars are brought together in a cluster (Scheme 1e) as the solvent evaporates after rinsing the modified surface with it, the exposed chemical functionalities (end groups) have a chance to interact—that is, to form bonds of different strengths—with either corresponding molecules or areas of the exposed nonfunctionalized surface on neighboring pillars, and thus to provide the basis for the adhesion forces that would govern the stability (or lack thereof) of the clusters after the solvent has evaporated. Depending on the number, type, and, ultimately, the total effective strength of the bonds that are formed, the balance between the resulting adhesion force  $A_1$  and the elastic force  $E$  in the absence of the capillary force  $C$  in the dried sample will determine whether the formed clusters disassemble fully (weak or no bonding,  $A_1 < E$ , Scheme 1f), disassemble partially (bonding of intermediate strength comparable to the elastic force,  $A_1 \approx E$ , Scheme 1g) or stay intact (strong bonding relative to the elastic force,  $A_1 > E$ , Scheme 1h). Thus, the clustering picture that results is a direct indication of the strength of the chemical bonds responsible for the macroscopically observed adhesive clusters and it provides a rough quantitative estimate of cluster stability as determined by the balance between  $A_1$  and  $E$ . Here, we take advantage of this property to investigate how a range of surface modifications, with different functional groups, chain lengths, and resulting expected bond strengths contributing to the macroscopic adhesion force, affect the stability of the clusters.

While gold-covered nonfunctionalized micropillar structures do not form clusters at any stage ( $C < E$ ), all chemically functionalized pillars assemble into  $2 \times 2$  groups before ethanol has fully evaporated ( $C > E$ ). Modeling the size of the clusters expected to form in our system (with its specific geometry, Young's modulus, and surface tension), using the quasi-static equation that balances elasticity with capillarity, indeed predicts the formation of such four-membered assemblies.<sup>19,21–23,25,34</sup> Such a prediction, however, is not sufficient for estimating the size of the final assemblies in real systems that can undergo disassembly upon drying due to insufficient adhesion between the assembled pillars. Indeed, while nearly complete surface coverage by four-pillar clusters in the dry state ( $C > E$  and  $A_1 > E$ ) was observed for micropillars functionalized with  $C_{10}$ -COOH (Figure 1 and 2f) and  $C_{11}$ -OH (Figure 2d), micropillars functionalized with  $C_{11}$ -CH<sub>3</sub> form ephemeral four-pillar clusters during ethanol evaporation ( $C > E$ ), which then fully disassemble (Figure 2i) ( $A_1 < E$ ). This result is independent of the method of functionalization (from solution, as in Method I, or the gas phase, as in Method II), which indicates that the surface molecule itself, regardless of the deposition method, is responsible for the increased clustering or disassembly and confirms that a simple surface modification can tip the balance between  $A_1$  and  $E$  in favor of either cluster stability or dissociation. These strikingly different stabilities of the clusters are consistent with the different types of bonds expected to predominate for each particular modifier molecule. The carboxylic groups of  $C_{10}$ -COOH are capable of forming hydrogen bonds, with a dissociation energy on the order of 6–8 kcal/mol per hydrogen bond,<sup>40</sup> while the alkyl chains of  $C_{11}$ -CH<sub>3</sub> can interact only by van der Waals forces that are less than 1 kcal/mol.<sup>40</sup> We note that these values are expected to hold for molecules in a monolayer; estimates of the strengths of hydrogen bonds between carboxylic acid end groups within a monolayer and of those between the carboxylic acid end group of a monolayer and an incoming probe molecule of a

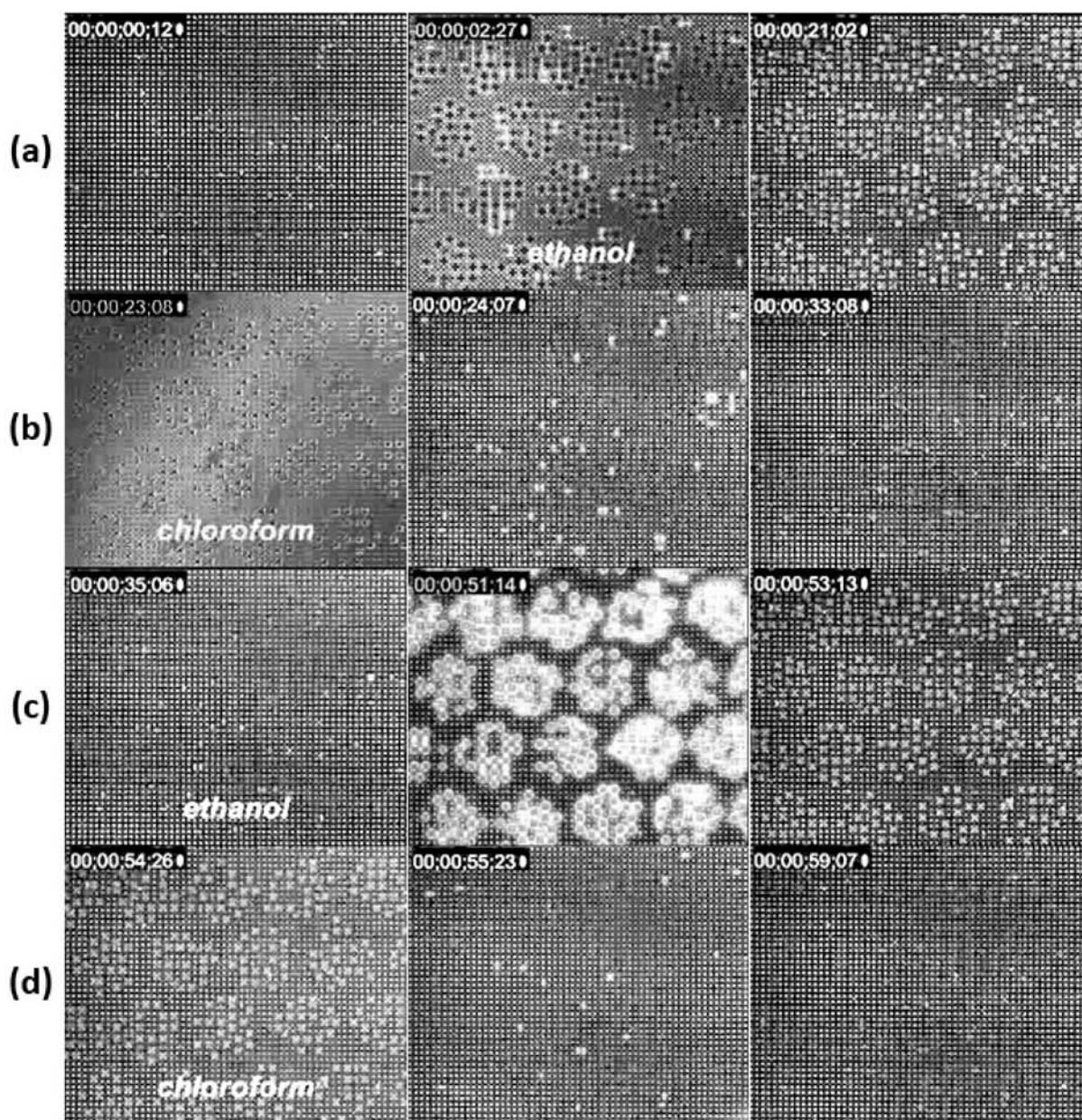


**Figure 5.** Still frames from the Supporting Movie 2<sup>38</sup> showing multiple cycles of reversible localized cluster formation and erasure in a micropillar array patterned with regions functionalized with C<sub>10</sub>-COOH. (a) Exposure to ethanol. Left to right: dry micropillar array with no clusters; capillarity-induced patterned clustering in the presence of ethanol; stable patterned clusters after evaporation of ethanol. (b) Exposure of the ethanol-clustered micropillar array to chloroform. Left to right: the array immediately after the exposure to chloroform; almost instantaneous full disassembly of the clusters in chloroform; dry, unclustered array after evaporation of chloroform. (c) Exposure of chloroform-unclustered array to ethanol. Left to right: the micropillar array immersed in ethanol; evaporation-induced patterned cluster formation in the presence of ethanol; stable, patterned clusters after evaporation of ethanol. (d) Second exposure of the ethanol-clustered micropillar array to chloroform. Left to right: the array immediately after the exposure to chloroform; almost instantaneous full disassembly of the clusters in chloroform; dry, unclustered array after evaporation of chloroform. Frame dimensions are 470  $\mu\text{m}$   $\times$  385  $\mu\text{m}$ .

carboxylic acid both fall in the range expected for solution-phase carboxylic acids: at least 7.2 kcal/mol<sup>41</sup> and  $\sim$ 7.5 kcal/mol/bond,<sup>42</sup> respectively.

Further proof that the cluster stability (that is, adhesion among/between the pillars) can be controlled by simply tuning the chemistry of the modifier molecules comes from additional comparisons among the different types of modifications. Notably, the functional group alone and the type of the bonds it can form with the neighboring pillars cannot fully explain the range of

stabilities observed in our system. In particular, the stabilities of clusters formed by pillars modified with short-chain OH-terminated molecules (Figure 2c, nearly complete disassembly,  $A_1 < E$ ) or short-chain COOH-terminated molecules (Figure 2e,  $\sim$ 25% stable clusters,  $A_1 \approx E$ ) are substantially inferior to those of their long-chain analogs. We attribute this difference to disorder of the SAMs of short-chain molecules on Au surfaces that would cause them to form a less ordered, lower-density, hydrogen-bonded surface network between the adjacent pillars and would thus decrease

the effective net adhesion force. Consequently, while adhesion between the OH- and COOH-terminated long-chain molecules exceeds the elastic force and leads to stable clusters, the effective net adhesion force generated between pillars functionalized with the short-chain molecules becomes comparable to or lower than the elastic force and leads to partial or complete disassembly.

Our observations indicate that, for the short-chain monolayer molecules, cluster stability parallels the order of the strengths of the chemical bonds that are at play:  $\text{H}\cdots\text{NH}_2 \approx \text{H}\cdots\text{OH} < \text{H}\cdots\text{O}=\text{COH} < \text{RS}-\text{SR}$  (or  $\text{RS}-\text{Au}$ ) or, in other words, the strength of the chemical bond involved is directly read out as the percentage of stable clusters observed in the samples. We interpret these results in the following way. Assuming comparable levels of disorder in the monolayers of short-chain molecules, the resulting stabilization of clustering (i.e., net adhesion force), though not very significant, is still quite pronounced only for  $\text{C}_2$ -COOH (~25% stable clusters) and  $\text{C}_2$ -SH (~35% stable clusters), which respectively form either fairly strong hydrogen bonds (6–8 kcal/mol/bond) or even stronger S–Au bonds (~44 kcal/mol<sup>43</sup>) or S–S covalent bonds (70–73 kcal/mol measured,<sup>44</sup> 50–65 kcal/mol calculated<sup>45</sup>). The fine balance between the comparable adhesive and elastic forces in these two systems and the resulting stability of individual clusters will be highly sensitive to the local disorder of these monolayers and local differences in the elasticity of the assembling pillars. This sensitivity further manifests itself in fairly high standard deviations in the measured percentages of stable clustering (Figure 1).

The case of dithiol-modified surfaces deserves further discussion. While pillars functionalized with longer-chain COOH- or OH-terminated thiols form highly stable clusters compared to their short-chain counterparts, the increase in the chain length of bifunctional dithiols from  $\text{C}_2$  (Figure 2g) to  $\text{C}_9$  (Figure 2h) results in an opposite effect. Due to the presence of two SH functionalities on the ends of the highly flexible  $\text{C}_9$ -hydrocarbon chain, the initial modification of the Au surface with  $\text{C}_9$ -SH results in high proportions of the molecules either bound at both ends to the same pillar<sup>46–48</sup> (Figure 1) or covalently bound to an adjacent SH functionality to form S–S bonds within a monolayer<sup>49</sup> prior to the clustering step. As a result, only very few unreacted SH groups remain available to form RS–SR covalent bonds or RS–Au surface bonds that would hold the pillars in a stable cluster. The looped  $\text{C}_9$ -SH molecules will instead expose the hydrocarbon chains, such that the adhesion between the pillars will be governed by weak van der Waals forces similarly to  $\text{C}_{11}$ - $\text{CH}_3$ -modified surfaces, and clusters will undergo full disassembly upon drying. Indeed, the contact angle values measured for the surfaces modified with  $\text{C}_2$ -SH,  $\text{C}_9$ -SH, and  $\text{C}_{11}$ - $\text{CH}_3$  ( $67^\circ \pm 10^\circ$ ,  $92^\circ \pm 11^\circ$ , and  $97^\circ \pm 3.4^\circ$ , Table 1) are in agreement with these observations and reasoning.

Overall, these results demonstrate that both the nature of the headgroup and the length of the hydrocarbon chain affect adhesion forces. By choosing an appropriate surface modifier, one can bias the assembling system toward complete dissociation of the clusters (e.g., by using  $\text{CH}_3$ -terminated surfaces), high cluster stability (e.g., by using functionalization with long-chain COOH-terminated thiols), or a wide range of intermediate stabilities.

**4.2. Modulating the Adhesion Forces by Solvents – toward Reversible Self-Assembly.** Yet another level of control over the stability or reversibility of the clustering process can be achieved through the exposure of the assembled surfaces to various solvents that can alter the bonding network and, consequently, the adhesion force between pillars (defined as  $A_2$  in

Scheme 1i, j). The stable clusters held together by the high adhesion force originating from hydrogen bonding ( $\text{C}_{11}$ -OH,  $\text{C}_2$ -COOH, and  $\text{C}_{10}$ -COOH-modified pillars) are easily disassembled by water or organic solvents such as ethanol, acetone, and chloroform (Scheme 1i). In sharp contrast, the clusters formed by  $\text{C}_2$ -SH-terminated pillars remain stable when exposed to these solvents (Scheme 1j), conceivably due to the covalent nature of the bonds involved.

In the former cases, the hydrogen bonds connecting the surfaces of the adjacent pillars are expected to be quickly replaced by hydrogen bonds with the solvent molecules for polar and protic solvents and to remain strong in nonpolar solvents. However, we observe that the clusters are highly unstable even in chloroform. Moreover, the rate of the dissociation of the clusters does not simply follow the order of polarity of the solvents. In fact, the disassembly rate decreases with the increase of the dielectric constant of the solvent: chloroform (fastest rate,  $\epsilon = 4.81$ )  $\gg$  acetone ( $\epsilon = 21.0$ ) > ethanol ( $\epsilon = 25.3$ )  $\approx$  water (slowest rate,  $\epsilon = 80.1$ ).<sup>39</sup> One possible explanation for these observations is that the solvents of low polarity, by interacting with the  $\text{CH}_2$  chains, quickly disturb the van der Waals forces between the chains, likely by penetrating first through the disordered regions of the monolayers, thus effectively destabilizing the geometrical integrity of the ordered surface hydrogen bonding networks<sup>41,50–52</sup> and ultimately weakening the adhesion forces between the pillars within a cluster. The protic and polar solvents, on the other hand, act by disturbing the fairly tightly connected hydrogen bonding networks themselves, which involves participating in multiple competitive equilibria within the networks, between the networks, and with themselves. The clusters are ultimately disassembled, but the rate of disassembly is slower. While we are continuing to investigate the effects of various solvents on the cluster stability, our current data show that the stability of the micropillar clusters can be controlled and tuned not only by the choice of surface modification but also by modulating their chemical environment and hence adhesion forces using solvents.

Importantly, after treatment with solvents that induce cluster disassembly, the clusters can be easily reformed by a second exposure to ethanol and drying (see Figure 5). This phenomenon provides a simple way to tune the balance between adhesion and elasticity in real time, enabling structures to be designed for dynamic, responsive behavior. Using this approach, the assembly/disassembly processes can be made reversible and switchable on or off on demand.

**4.3. Spatial and Temporal Control of Adhesion – Reversible Area-Selective Clustering.** Several nano/microprinting technologies such as microcontact printing<sup>53,54</sup> and dip-pen lithography<sup>55</sup> have been developed to locally modify surface chemistry at the nano- or microlevel. Here, we capitalize on the results above and demonstrate *reversible area-selective assembly* by combining surface-chemistry-induced clustering with microcontact printing.

The patterned clustering is enabled by local modification of the surfaces with the molecules that produce extremely stable assembled clusters. The rest of the surface can either remain unfunctionalized Au or be modified with a methyl-terminated SAM. As seen in Figure 4, by stamping certain areas with  $\text{C}_{10}$ -COOH, we can easily achieve precise geometrical control over which parts of the microstructured surface will and will not undergo clustering. We can, of course, vary the shape and size of the stamp widely, thus enabling an exceptional level of control

over the geometrical aspect of cluster distribution. Even more importantly, we can erase the clustering pattern by rinsing with chloroform and then regenerate it again by treatment with ethanol. This reproducible, reversible switching between erasure and regeneration of the patterned clusters, shown in Supporting Movie 2<sup>38</sup> and Figure 5, demonstrates just a proof of concept, with any number of variations on the theme possible. One can envision a whole variety of areas stamped with different inks resulting in different cluster stabilities, as well as a variety of solvents added to different parts of the surface at different times, making the level of control over the assembly/disassembly process almost limitless.

## 5. CONCLUSIONS

This study demonstrates that chemical adhesion forces play a critical role in determining the stability of self-assembled clusters of micropillars, such that simple modifications of the surface chemistry allow the assemblies to be tuned for nearly any degree of reversibility and selective assembly/disassembly. Significantly, a change in the solvent environment can dramatically alter the molecular interaction, thereby switching very quickly, sometimes instantly, between the stable clusters and fully disassembled pillars. By combining a micropatterning technique with these simple chemical controls of the assembly process, area-selective formation, erasure, and regeneration of dynamic clusters were demonstrated. These results indicate that the strength of molecular interactions coded on the surface is straightforwardly translated into that of the pillar assembly. Thus, while the balance between capillarity and elasticity determines the *original* cluster size the system can reach in the wet sample, the balance between adhesion and elasticity determines whether this or lower-order assembly will be preserved in the final structure in the dry state.

The role of chemical adhesion has previously been discussed for molecular-scale self-assembly, but not for self-assembly at the mesoscale, where the balance between both the mechanical (elastic) and chemical properties of the building blocks determines their interactions. This study therefore provides fundamental insight into the mechanism of dynamic assembly and a straightforward strategy to develop bioinspired, responsive, reversible self-assembled systems.

One can envision a whole host of applications of these phenomena. For example, COOH-modified nano/microparticles can chemically bridge COOH-modified pillars, be captured by the assembling clusters, and be released upon immersion in appropriate solvents that minimize and ultimately overcome adhesive interactions. Such properties as the timing of particle release can be optimized by surface-chemistry-based stability and can be made responsive to solvent-induced changes. We believe that such a surface-modified capture–release system can be adapted for use in drug delivery. Reversible assembly/disassembly of micropillars will also determine the adhesive properties of materials or their optical properties (color, opacity, transmission), offering the foundation for the development of a new generation of dynamic materials.

## ■ ASSOCIATED CONTENT

Supporting Information. Movie 1. Capillarity-induced clustering of an array of micropillars modified with 1-Dodecanethiol (SH(CH<sub>2</sub>)<sub>11</sub>CH<sub>3</sub>) in ethanol and its full disassembly upon drying. Movie 2. Reversible area-selective clustering of an array of

micropillars patterned with regions bearing 11-Mercaptoundecanoic acid (SH(CH<sub>2</sub>)<sub>10</sub>COOH) SAM. The C<sub>10</sub>-COOH functionalized regions self-assemble into stable clusters in ethanol and then disassemble upon exposure to chloroform. This material is available free of charge via the Internet at <http://pubs.acs.org>.

## ■ AUTHOR INFORMATION

### Corresponding Author

jaiz@seas.harvard.edu

## ■ ACKNOWLEDGMENT

This work was supported by the DOE under Award DE-SC0005247. We acknowledge the use of the facilities at the Harvard Center for Nanoscale Systems supported by NSF Award No. ECS-0335765. We thank Prof. L. Mahadevan for insightful discussions and Dr. A. Grinthal for support with the manuscript preparation. M.M. acknowledges the partial financial assistance by the Marubun Research Promotion Foundation.

## ■ REFERENCES

- (1) Whitesides, G. M.; Grzybowski, B. *Science* **2002**, *295*, 2418–2421.
- (2) Gouaux, E.; Mackinnon, R. *Science* **2005**, *310*, 1461–1465.
- (3) Toyoshima, C.; Mizutani, T. *Nature* **2004**, *430*, 529–535.
- (4) Toyoshima, C.; Nomura, H. *Nature* **2002**, *418*, 605–611.
- (5) Oldham, M. L.; Khare, D.; Quijcho, F. A.; Davidson, A. L.; Chen, J. *Nature* **2007**, *450*, 515–521.
- (6) Hvorup, R. N.; Goetz, B. A.; Niederer, M.; Hollenstein, K.; Perozo, E.; Locher, K. P. *Science* **2007**, *317*, 1387–1390.
- (7) Hollenstein, K.; Frei, D. C.; Locher, K. P. *Nature* **2007**, *446*, 213–216.
- (8) Gao, X. F.; Jiang, L. *Nature* **2004**, *432*, 36.
- (9) Xia, F.; Jiang, L. *Adv. Mater.* **2008**, *20*, 2842–2858.
- (10) Autumn, K.; Liang, Y. A.; Hsieh, S. T.; Zesch, W.; Chan, W. P.; Kenny, T. W.; Fearing, R.; Full, R. J. *Nature* **2000**, *405*, 681–685.
- (11) Eisner, T.; Aneshansley, D. J. *Proc. Natl. Acad. Sci. U.S.A.* **2000**, *97*, 6568–6573.
- (12) Arzt, E.; Gorb, S.; Spolenak, R. *Proc. Natl. Acad. Sci. U.S.A.* **2003**, *100*, 10603–10606.
- (13) Gorb, S. N.; Sinha, M.; Peressadko, A.; Daltorio, K. A.; Quinn, R. D. *Bioinspiration Biomimetics* **2007**, *2*, S117–S125.
- (14) Abou Alaiwi, W. A.; Lo, S. T.; Nauli, S. M. *Sensors* **2009**, *9*, 7003–7020.
- (15) Bisgrove, B. W.; Yost, H. J. *Development* **2006**, *133*, 4131–4143.
- (16) Ibanez-Tallon, I.; Heintz, N.; Omran, H. *Hum. Mol. Genet.* **2003**, *12*, R27–R35.
- (17) Palmer, A. R. *Science* **2004**, *306*, 828–833.
- (18) Singla, V.; Reiter, J. F. *Science* **2006**, *313*, 629–633.
- (19) Bernardino, N. R.; Dietrich, S. *ACS Appl. Mater. Interfaces* **2010**, *2*, 603–604.
- (20) Bico, J.; Roman, B.; Moulin, L.; Boudaoud, A. *Nature* **2004**, *432*, 690.
- (21) Boudaoud, A.; Bico, J.; Roman, B. *Phys. Rev. E* **2007**, *76*, 060102.
- (22) Chandra, D.; Yang, S. *Acc. Chem. Res.* **2010**, *43*, 1080–1091.
- (23) Chandra, D.; Yang, S.; Soshinsky, A. A.; Gambogi, R. J. *ACS Appl. Mater. Interfaces* **2009**, *1*, 1698–1704.
- (24) Chen, R.; Lu, M. C.; Srinivasan, V.; Wang, Z.; Cho, H. H.; Majumdar, A. *Nano Lett.* **2009**, *9*, 548–553.
- (25) Chiodi, F.; Roman, B.; Bico, J. *Europhys. Lett.* **2010**, *90*, 44006.
- (26) De Volder, M.; Tawfick, S. H.; Park, S. J.; Copic, D.; Zhao, Z. Z.; Lu, W.; Hart, A. J. *Adv. Mater.* **2010**, *22*, 4384–4389.
- (27) Duan, H. G.; Berggren, K. K. *Nano Lett.* **2010**, *10*, 3710–3716.
- (28) Geim, A. K.; Dubonos, S. V.; Grigorieva, I. V.; Novoselov, K. S.; Zhukov, A. A.; Shapoval, S. Y. *Nat. Mater.* **2003**, *2*, 461–463.



- (29) Kang, S. H.; Pokroy, B.; Mahadevan, L.; Aizenberg, J. *ACS Nano* **2010**, *4*, 6323–6331.
- (30) Kim, H. Y.; Mahadevan, L. *J. Fluid Mech.* **2006**, *548*, 141–150.
- (31) Lau, K. K. S.; Bico, J.; Teo, K. B. K.; Chhowalla, M.; Amaratunga, G. A. J.; Milne, W. I.; McKinley, G. H.; Gleason, K. K. *Nano Lett.* **2003**, *3*, 1701–1705.
- (32) Pokroy, B.; Kang, S. H.; Mahadevan, L.; Aizenberg, J. *Science* **2009**, *323*, 237–240.
- (33) Py, C.; Bastien, R.; Bico, J.; Roman, B.; Boudaoud, A. *Europhys. Lett.* **2007**, *77*, 44005.
- (34) Zhao, Y. P.; Fan, J. G. *Appl. Phys. Lett.* **2006**, *88*, 103123.
- (35) Lu, Y.; Huang, J. Y.; Wang, C.; Sun, S. H.; Lou, J. *Nat. Nanotechnol.* **2010**, *5*, 218–224.
- (36) Pokroy, B.; Epstein, A. K.; Persson-Gulda, M. C. M.; Aizenberg, J. *Adv. Mater.* **2009**, *21*, 463–469.
- (37) Paulose, J.; Nelson, D. R.; Aizenberg, J. *Soft Matter* **2010**, *6*, 2421–2434.
- (38) See Supporting Information
- (39) Wohlfarth, C. In *CRS Handbook of Chemistry and Physics*, 91 ed.; Haynes, W. M., Ed.; CRC Press: 2010–2011; pp 186–190.
- (40) March, J. *Advanced Organic Chemistry*, 4 ed.; Wiley: 1992; pp 75–76.
- (41) Cooper, E.; Leggett, G. J. *Langmuir* **1999**, *15*, 1024–1032.
- (42) Sun, L.; Kepley, L. J.; Crooks, R. M. *Langmuir* **1992**, *8*, 2101–2103.
- (43) Dubois, L. H.; Nuzzo, R. G. *Annu. Rev. Phys. Chem.* **1992**, *43*, 437–463.
- (44) Franklin, J. L.; Lumpkin, H. E. *J. Am. Chem. Soc.* **1952**, *74*, 1023–1026.
- (45) Jursic, B. S. *Int. J. Quantum Chem.* **1997**, *62*, 291–296.
- (46) Akkerman, H. B.; Kronemeijer, A. J.; van Hal, P. A.; de Leeuw, D. M.; Blom, P. W. M.; de Boer, B. *Small* **2008**, *4*, 100–104.
- (47) Kohale, S.; Molina, S. M.; Weeks, B. L.; Khare, R.; Hope-Weeks, L. J. *Langmuir* **2007**, *23*, 1258–1263.
- (48) Qu, D.; Kim, B. C.; Lee, C. W. J.; Uosaki, K. *Bull. Korean Chem. Soc.* **2009**, *30*, 2549–2554.
- (49) Liang, J.; Rosa, L. G.; Scoles, G. *J. Phys. Chem. C* **2007**, *111*, 17275–17284.
- (50) Dubois, L. H.; Zegarski, B. R.; Nuzzo, R. G. *J. Am. Chem. Soc.* **1990**, *112*, 570–579.
- (51) Nuzzo, R. G.; Dubois, L. H.; Allara, D. L. *J. Am. Chem. Soc.* **1990**, *112*, 558–569.
- (52) Smith, E. L.; Alves, C. A.; Anderegg, J. W.; Porter, M. D.; Siperko, L. M. *Langmuir* **1992**, *8*, 2707–2714.
- (53) Gates, B. D.; Xu, Q.; Stewart, M.; Ryan, D.; Willson, C. G.; Whitesides, G. M. *Chem. Rev.* **2005**, *105*, 1171–96.
- (54) Qin, D.; Xia, Y.; Whitesides, G. M. *Nat. Protoc.* **2010**, *5*, 491–502.
- (55) Ginger, D. S.; Zhang, H.; Mirkin, C. A. *Angew. Chem., Int. Ed.* **2004**, *43*, 30–45.